Faraday Discussions
Cite this: *Faraday Discuss.*, 2015, **180**, 205

Corrosion scales and passive films: general discussion

Gerald Frankel, Janine Mauzeroll, Geoffrey Thornton, Hendrik Bluhm, Jonathan Morrison, Vincent Maurice, Trevor Rayment, David Williams, Angus Cook, Gaurav Joshi, Alison Davenport, Simon Gibbon, Denis Kramer, Matthew Acres, Markus Tautschnig, Hiroki Habazaki, Philippe Marcus, David Shoesmith, Clara Wren, Tom Majchrowski, Rob Lindsay, Mary Wood, Mira Todorova, John Scully, Frank Renner, Anton Kokalj, Christopher Taylor, Sannakaisa Virtanen and Julian Wharton

DOI: 10.1039/c5fd90045j

Sannakaisa Virtanen opened a general discussion of the paper by Mira Todorova: In view of the fact that there is a lot of data available for ZnO (as a semiconducting oxide), how "easy or difficult" is it to use the same methodology for other oxides, such as for instance iron oxides or chromium oxide? What experimental data would be needed for some validation of the calculations?

Mira Todorova replied: There is no principle problem in applying the methodology to other oxides, *i.e.* iron oxides or chromium oxides. The question boils down to the availability of the relevant defect data. ZnO was a great oxide to consider as an example, because it is of interest to both the corrosion and the semiconducting community. Thus, there were already a lot of data available for ZnO. What we would now need to do is to expand on the available database of *ab initio* calculations for charged point defects in other oxides or materials of interest in the context of corrosion. Unfortunately, there is little, if any, such information available for most of the oxides which are interesting in the context of corrosion. Furthermore, some of the most interesting oxides in the context of corrosion, such as the iron or chromium oxides, are unfortunately very challenging for *ab initio* calculations, as they possess strong electronic correlations. This means that the required calculations are not just "routine calculations", which can be performed in a high-throughput fashion.

There are various experiments that can be performed to obtain information about the point defects present in a system, such as DLTS (deep level transient spectroscopy), Hall measurements, EPR, *etc.* A general discussion about the comparison of the discussed defect calculations to experiment can be found in ref. 1. A discussion focusing on the experimental identification of the discussed native point defects in ZnO can be found in ref. 2.

1 C. G. Van de Walle and J. Neugebauer, *J. Appl. Phys.*, 2004, **95**, 3851.
2 A. Janotti and C. G. Van de Walle, *Rep. Prog. Phys.*, 2009, **72**, 126501.

Philippe Marcus asked: If the defects are neutral, one would expect no effect of the electric field on oxide growth. Is this what you suggest?

Mira Todorova responded: This is a very interesting suggestion to experimentally verify the existence/presence of charge neutral defects. We have not considered this aspect in our paper but would like to call for corresponding experiments in the region of phase space where such defects are predicted to be thermodynamically stable.

Hendrik Bluhm questioned: Have you considered the presence of a hydroxide phase at the interface between ZnO and water? How would the presence of the hydroxide phase influence your model on the role of point defects in governing the growth/dissolution of the oxide formed on Zn?

Mira Todorova answered: A hydroxide phase at the interface was not considered. We chose ZnO for two reasons: (i) because of the availability of a vast amount of relevant data found for ZnO in the semiconductor literature and (ii) because ZnO is mentioned in the experimental literature on corrosion, as being the first compact oxide layer formed during corrosion on ZnO.[1] The methodology presented in our work can be equally well applied to a hydroxide phase. Unfortunately, to our knowledge the information about the point defects forming in a Zn-hydroxide, which is needed for our thermodynamic model, is not available in the literature yet. Once we have performed the necessary density-functional theory calculations for the point defects in the hydroxide phase, the presence of the hydroxide phase can be explicitly considered.

1 S. Thomas, *et al.*, *Electrochimica Acta*, 2013, **97**, 192.

Gerald Frankel asked: Regarding the neutral defects, are the electrons or holes kept localized to the vacancies by electrostatic interaction?

Mira Todorova replied: The neutral defects are true bonding states. A comprehensive study of the electronic and geometric structure of these defects can be found in ref. 1 (for the oxygen split interstitial defect O_i^0 (split)) and in ref. 2 (for the oxygen vacancy V_O^0). Following are briefly some of the main points, regarding the bonding nature of these defects, as found in the mentioned publications.

In the O_i^0 (split) configuration two oxygen atoms share a lattice site and form a bond of length 1.46 Å with each other. This leads to the appearance of two almost degenerate states in the band bap, which are completely filled. The electronic configuration of this defect resembles an antibonding ppπ* molecular state found in an isolated O_2 molecule.

The oxygen vacancy defects involve 4 Zn dangling bonds (sp^3-hybrids) and two electrons. The Zn dangling bonds combine to a fully symmetric a_1 state located in the band gap and three almost degenerate states in the conduction band. For the neutral oxygen vacancy, the a_1 state is fully occupied by two electrons.

1 A. Janotti and C. G. Van de Walle, *Phys. Rev. B: Condens. Matter Mater. Phys.*, 2007, **76**, 165202.
2 A. Janotti and C. G. Van de Walle, *Rep. Prog. Phys.*, 2009, **72**, 126501.

Christopher Taylor enquired: The "Pourbaix diagram" for point-defects shows the regions of E_h–pH space subdivided, according to which point-defect has the lowest free energy of formation. However, I was wondering if it is not impossible for multiple types of point-defect to co-exist in the same domains, if they both have negative free energies?

Mira Todorova responded: Having a negative free energy of formation is not a prerequisite for the existence of a defect. Usually the reason for the presence of defects in a material is configurational entropy, not an exothermic formation enthalpy at $T = 0$ K. The defects shown in the defect stability phase diagram (Fig. 3 in our paper) are the dominant defect in the system, *i.e.* the defects which will be present in high concentration at the conditions at which they have the lowest formation energy. Thus, indeed the presence of other defects within the system is not excluded and various defects may coexist. Fig. 2 in our paper shows all the possible native defects within the ZnO system. There are various conditions, at which defects, other than the ones appearing in the defect stability phase diagram, have formation energies not much higher than the formation energies of the respective dominant defect. The likelihood and concentration in which such defects will be found in the system at the given conditions can be calculated using their formation energy at the conditions of interest and eqn (1).

Christopher Taylor asked: Is it possible to construct a point-defect phase diagram when the oxide film has more than one metallic element and/or the oxide film is formed over an alloy?

Mira Todorova answered: Yes, it is straight forward to construct defect phase diagrams for systems containing more than two elements. The methodology remains unchanged and allows to consider any number of elements. The only difference will be that such a diagram will no longer be 2-dimensional but must reflect the number of chemical species that can change independently.

John Scully commented: Thank you for your clarification that your map shows the most stable defect from the thermodynamic view and that there might be other "less stable" defects at a lower concentration which co-exists.

I have two questions. How do you rationalize experiments on oxide growth that suggest "transference number" or that many oxides grow by a combination of cations moving out and anions in? Marker studies indicate this and that experimental conditions can be changed to alter this behavior.

The second question regards the role of metastable point defects and the higher disordered state of passive films when they first begin to thicken. How should we think about these? Couldn't these metastable point defects be dominant factors early in growth?

Mira Todorova replied: Based on Fig. 2 in our paper I would conclude that, at the conditions relevant when ZnO comes into contact with water, all the

metastable defects are rather high in energy to be expected to play any significant role. However, one should keep in mind that the model system we use here is still rather simple compared to the complexity of the oxide films formed in a corrosive environment. Therefore, a next step would be to expand this defect picture to the consideration of defects in the subsurface and surface region of the oxide as well as to include diffusion barriers.

Clara Wren remarked: Your calculations assume that ZnO is a relatively pure semi-conductor except for the small density of defects that you introduce. On a corroding surface, the oxide layer is not likely a uniform layer but will have a distribution of ions and ion vacancies. Thus, the electron energy at the metal/oxide interface is near the energy of the conduction band energy while that at the oxide/water interface is near the valence band energy. Since your model shows stability regions for different defects, could your model be used in predicting the kinetics of oxide growth?

Mira Todorova responded: You are, of course, correct that the oxide at the corroding surface will be much more complex than the rather perfect oxide assumed in our theoretical approach. Such a simple model will not be able to capture the whole complexity of the corrosion product. The consideration of the charged bulk point defects presents a first step, which provides some insight into the system and forms a solid basis which we can expand on in future. An obvious next step would be to explicitly include the presence of a surface/interface and investigate sub-surface and surface defects. While the model allows identifying trends, without knowledge of at least the migration barriers it is difficult to predict the kinetics of the oxide growth.

David Williams addressed Mira Todorova and Clara Wren: I'm interested to explore the connection of your defect stability diagrams to measurements of dependence of current density on applied electrode potential. The paper by Momeni and Wren is also relevant to this discussion, as they discuss that the potential difference between metal and solution is distributed across the two interfaces (metal–oxide and oxide–solution) and across the oxide film. The dependence on interfacial potential difference of the current flow across the interfaces can be described by a Butler–Volmer equation. The dependence of the current on the potential difference across the film can be described by a high-field growth law (Cabrera–Mott) or its linear low-field limit in which, of course, the charge on the migrating defect appears. The potential profile across the system can be drawn onto the diagram of μ_O against E_F where at least the end points (metal and solution) are known, and the path then drawn depends on assumptions about the potential differences across the interfaces and the electric field in the oxide film, and whether there are any composition variations (space charges) developed in the oxide near the interfaces. Where this path goes will determine the dependence of the current on the field in the oxide, through the charge on the migrating defects, and since the current is continuous it will then determine the magnitude of the potential differences across the interfaces. There ought to be a self-consistent solution which can be mapped onto experimental data, similar to the procedure used by Momeni and Wren. Could you comment?

Mira Todorova answered: This is an interesting suggestion, but requires additional conceptual development in order to include the potential profile and connect our defect stability diagrams with the Cabrera–Mott model. It is a point we will consider in the future.

Clara Wren commented: This question is primarily addressed to Dr. Mira Todorova. My comment on the discussion on defect stability regions is that Dr. Todorova's model, which shows stability regions for different defects, further confirms our assumptions regarding a corroding system. On a corroding surface, the oxide layer is not likely a pure semi-conductor, but will have a distribution of ions and ion vacancies, and the electron energy at the metal/oxide interface is near the energy of the conduction band energy while that at the oxide/water interface is near the valence band energy.

Philippe Marcus asked: The energy of defect formation is certainly an important factor, but dont't you think that the energy barrier (and hence activation energy) for the migration of defects is also very important for oxide growth?

Mira Todorova responded: Yes, indeed. The energy barrier for the migrations of defects is a very important parameter, which needs to be considered. The thermodynamic aspect we consider here should be regarded only as a first step towards modelling the oxide growth. Specifically, this step provides information about the (thermodynamically) dominant defects and about gradients. Whether these gradients can be realised will depend on the kinetics in the system.

In the semiconducting literature mainly the energetic position of the defect levels are of interest since this controls the electronic behaviour of the material. Consequently, there is a lot of data available about defect formation energies and different charged states (for materials of interest in this field), since these quantities yield information about the charge transition levels. Data on diffusion barriers is much sparser. Some information about the migration of oxygen and zinc defects in ZnO can be found in ref. 1, albeit at the LDA+U level.

The application and usefulness of such an *ab initio* derived methodology in corrosion science requires that the calculation of quantities like defect formation energies and migration barriers is pursued much more vigorously in the future, in particular for materials interesting in the context of corrosion.

1 A. Janotti and C. G. Van de Walle, *Phys. Rev. B: Condens. Matter Mater. Phys.*, 2007, **76**, 165202.

Denis Kramer queried: Do the supercell calculations of the neutral defects, especially the neutral oxygen vacancy, yield semi-conducting states with a band gap?

Mira Todorova said: Yes, the point defects yield semi-conducting states in the band-gap. The band structures for the perfect ZnO crystal, the neutral oxygen vacancy and 2+ oxygen vacancies, calculated with the HSE-functional, are shown in Fig. 3 of ref. 1. A discussion of the electronic structure of the oxygen vacancy (in its various charged states) can also be found in ref. 2.

1 F. Oba, A. Togo, I. Tanaka, J. Paier and G. Kresse, *Phys. Rev. B: Condens. Matter Mater. Phys.*, 2008, **77**, 245202.
2 A. Janotti and C. G. Van de Walle, *Rep. Prog. Phys.*, 2009, **72**, 126501.

Philippe Marcus asked: To what extent do the boundaries between stability domains of defects change if different hybrid functionals are used?

Mira Todorova responded: This is a very interesting and relevant question. Unfortunately, there are as yet no systematic investigations, which would allow us to give a general answer to this question. It is something that definitely needs to be investigated, since it will allow us to assess the accuracy we can achieve.

Simon Gibbon enquired: At the end of the penultimate paragraph of your paper you state that "this insight may be used to identify new strategies towards improving corrosion protection." Please could you explain what new strategies you envision?

Mira Todorova replied: The possibility to use a defect stability phase diagram to identify the defects relevant in the context of oxide growth and quantify the regions within which they are stable opens the door to perform systematic searches for alloying elements/dopants which may (i) make ZnO more intrinsic, *i.e.* shift the Fermi level towards p-type conditions, and (ii) prevent the formation of a defect, which has been identified as being harmful, or bind it by forming some complex, which prevents its migration.

Tom Majchrowski communicated: An interesting model is proposed, but how would it respond to the presence of alloying elements and/or impurities?

Mira Todorova communicated in reply: There is no fundamental difference between the treatment of charged point defects native to the considered oxide or charged point defects stemming from alloying elements and/or impurities within the proposed method. In the context of semiconductors, defects due to elements alien to the semiconductor are dopants and a subject of investigation. A brief glance at the ZnO literature revealed that there are, for example, first principles calculations for hydrogen,[1] nitrogen,[2] or Si and Ge[3] already available. It would be straight forward to use this information when constructing the defect stability phase diagram for ZnO. The configurational space which needs to be considered by the inclusion of dopants (impurities, alloying elements) increases and there is also always the question of availability of existent calculations for the impurity of interest.

1 A. Janotti and C. G. Van de Walle, *Rep. Prog. Phys.*, 2009, **72**, 126501.
2 J. L. Lyons, A. Janotti, and C. G. Van de Walle, *Appl. Phys. Lett.*, 2009, **95**, 252105.
3 J. L. Lyons, A. Janotti, and C. G. Van de Walle, *Phys. Rev. B: Condens. Matter Mater. Phys.*, 2009, **80**, 205113.

Rob Lindsay asked: Could you please clarify the charge removed/remaining upon creation of the various point defects (*e.g.* the neutral oxygen vacancy)?

Mira Todorova responded: Each Zn(O) atom in ZnO is tetrahedrally coordinated. The way in which chemists and semiconductor physicist think about the

building blocks of ZnO is conceptually different, although both of course describe the same material system. In the chemical community ZnO is thought of as being built by Zn^{2+} and O^{2-} ions. In semiconductor physics each of the Zn(O) forms polarized covalent bonds with its 4 O(Zn) neighbours (sp^3-hybrides). A Zn atom contributes ½ electron to each of these bonds (the 2 Zn valence electrons are distributed onto 4 bonds) and an O atom contributes $^3/_2$ electrons to each bond (the 6 O valence electrons are distributed onto the 4 bonds). When an O atom is removed to form an oxygen vacancy 4 unpaired Zn dangling bonds remain, which can be filled with up to 2 electrons. In the case of a neutral oxygen vacancy, V_O^0, a neutral oxygen atom is removed from the lattice and the remaining 2 electrons of the Zn have to be distributed onto the Zn dangling bonds. The corresponding electronic structure was already touched upon in the answer to Prof. Frankel. When the oxygen vacancy is in the +1 charged state, V_O^{1+}, a O^{1-} ion has been removed from the lattice. One electron remains, which can be distributed onto the four Zn dangling bonds. This is 1 electron short of the maximum occupation possible within a covalent bond. When the oxygen vacancy is in the +2 charged state, V_O^{2+}, a O^{2-} ion has been removed from the lattice and all Zn dangling bonds are empty. The relaxation patterns found for each of these defects can be seen in Fig. 5 of ref. 27 mentioned in our paper, as well as a discussion of the electronic structure of these defects.

Anton Kokalj communicated: It is not clear to me how you align the levels (bands) in respect to the vacuum level. Namely, the position of the energy levels (in respect to the vacuum level) inside the material depends on the conditions at the surface (*e.g.*, type of surface termination, *etc.*). However, the "surface details" seem not to enter into your formalism.

Mira Todorova communicated in reply: The surface/interface dipole is indeed important in the context of alignment. Although this is not an aspect we mention explicitly in the paper, indirectly it is considered in Fig. 4(b) of our paper, where you may notice the two jumps in the vacuum level (at the positions of the interface) of the system after equilibration.

Specifically, we used the work function of Zinc to align the Fermi level of the metal on an absolute scale. For the purpose of this work differences in the work function, due to the orientation of the sample (which are typically small) as well as due to the formation of surface dipoles, were not considered, but can be easily included. To align the ZnO and water levels we used the universal alignment, which was found to exist for the hydrogen (±) transition level in semiconductors, insulators and water.[1] Based on the calculations we used, we would consider this alignment to be accurate within 0.2–0.3 eV. Our recent work allowed us to rationalize the standard hydrogen electrode on a microscopic level.[2] There, we also discuss the alignment of the $H^{+(aq)}$ and $OH^{-(aq)}$ defects and the hydrogen (±) level in water on an absolute scale.

1 C. G. Van de Walle and J. Neugebauer, *Nature*, 2003, **423**, 626.
2 M. Todorova and J. Neugebauer, *Phys. Rev. Applied*, 2014, **1**, 014001.

Jonathan Morrison opened the discussion of the paper by Clara Wren: Alloy 800 and Stellite are generally found in high temperature water environments;

have you compared your model output to literature data for oxide films formed under the expected service conditions? Has the model still proven to be successful?

Clara Wren answered: We have not yet applied our model to such high temperatures (in the range 250–320 °C), but we are planning to do so. We have used our model to simulate our corrosion experiments on a range of Fe–Ni–Cr and Co–Cr alloys performed at temperatures up to 150 °C. In these studies, we have performed both coupon corrosion tests and potentiostatic polarization experiments combined with post-test surface and solution analyses (ref. 15, 16, and 21 in our paper). The MCB model simulates the current as a function of time, the composition and layer structure of the oxides formed, and the amounts of dissolved metals well. More importantly, the best-fit model parameters have expected temperature dependences, indicating that the model can predict the effect of temperature.

David Shoesmith asked: Can your model predict the influence of temperature on film composition and thickness? Experimental observations show that the passive current does not change much with temperature (at least over the range 25 °C to 90 °C). Our experiments indicate the current is controlled by a combination of decreased Cr content (which should increase the current) which is counterbalanced by an increased thickness.

Clara Wren answered: Yes, our model can predict the effect of temperature on film composition and thickness. As noted in our response to the earlier question by Dr J. J. Morison, we have applied our model to temperatures of up to 150 °C. The MCB model simulations results are in good agreement with the experimental data (the current as a function of time, the composition and layer structure of the oxides formed, and dissolved amounts of different metals) obtained at all of the temperatures studied so far. More importantly, the best-fit model parameters show expected temperature dependences. In the MCB model, the rate constants for oxide formation and dissolution depend on temperature. The first-order rate constant for oxide formation will increase with temperature according to an Arrhenius dependence, while that for dissolution will have a more complicated temperature dependence (due to increasing rate constants for surface hydration and hydrolysis reactions and typically non-linear dependences of the solubilities of metal cation species on temperature). In our experimental studies we found that a Fe–Ni–Cr alloy forms an oxide with a mixed spinel oxide ($FeCr_2O_4$/Fe_3O_4/$NiFe_2O_4$) inner layer and a NiO/$Ni(OH)_2$ outer layer. The outer layer thickness increases with increasing temperature and this results in a decrease in Cr content of the oxide.

Janine Mauzeroll queried: Could you further explain the weighing that was applied for the water and oxygen reaction that concomitantly also occurs at the working electrode?

Clara Wren answered: The reduction reactions of H_2O or dissolved O_2 (at an impurity level) on the working electrode are coupled with oxidation of H_2 or H_2O on the counter electrode (reactions (1)–(4)):

$$2H_2O + 2e^- \rightarrow H_2 + 2OH^- \text{ on WE} \quad (1)$$

$$H_2 + 2OH^- \rightarrow 2H_2O + 2e^- \text{ on CE} \quad (2)$$

and/or

$$O_2 + 2H_2O + 4e^- \rightarrow 4OH^- \text{ on WE} \quad (3)$$

$$4OH^- \rightarrow O_2 + 2H_2O + 4e^- \text{ on CE} \quad (4)$$

These aqueous redox reactions do not contribute to the metal oxidation flux or oxide growth flux, but to the net current that is being monitored during polarization. Thus, in order to compare the model results with experimentally measured quantity current, we take into account the contribution of the solution reduction on the WE to the current. This solution reduction reaction is treated as a separate independent redox reaction with its own equilibrium potential (or the difference of the equilibrium potentials of the two half-reactions of aqueous reduction and aqueous oxidation).

In the simulation of the potentiostatic polarization experiments on Stellite-6 and Alloy 800, the solution reduction reaction on the WE is represented by one reaction:

$$Ox(s) + ne^- \rightarrow Red(s) + \text{ on WE} \quad (5)$$

The solution reduction flux was modelled in the same way as the metal oxidation flux, *i.e.*, using a modified Butler–Volmer equation with an effective overpotential:

$$J_{sol-red}(t)|_{ox|sol} = -J^{eq}_{sol-rdx}\exp\left(\frac{0.5nF}{RT}\left(-\eta^{eff}_{sol-red}\right)\right) \quad when\ \eta^{eff}_{ox\#}(t) < 0 \quad (6)$$

$$\eta^{eff}_{ox\#}(t) = E^{eq}_{sol-red} - E^{elec} - f_{sol}\Delta V_{oxide} \quad (7)$$

where $E^{eq}_{sol-red}$ is the equilibrium potential for the solution redox reaction, and the factor f_{sol} is used to adjust for the difference in the potential barrier for the electron transfer for solution redox reactions and for ion and ion vacancy transfer for metal/metal oxide redox reactions.

Since the potential drop for the cathodic reaction is several orders of magnitude lower than that of the anodic reaction, and it is negligible in comparison to that of anodic reaction, f_{sol} is assumed to be zero. Due to a difficulty in accurately measuring the dissolved concentrations of H_2, O_2 and possibly other redox active impurities, $E^{eq}_{sol-red}$ was obtained by measuring the open circuit potential on a Pt working electrode in the same solution environment. In the Ar-purged solution at pH 10.6 the open circuit potential was measured to be 0.2 V_{SCE}.

Philippe Marcus enquired: Why do you consider only the flux of cations in the oxide?

What are the possible rate-determining steps and the values of the physical parameters needed to calculate real kinetics of oxide growth?

Clara Wren replied: We have considered the fluxes of different charged species, metal cations, oxygen anions and their vacancies and electrons and holes in the oxide. However, as stated in the paper, we have concluded that detailed modeling of the fluxes of individual charged species is not necessary because their fluxes cannot vary independently due to mass and charge conservation requirements. What is strictly observed in our MCB (mass and charge balance) model is that the flux of cations created by oxidation (referred to as the oxidation flux in the paper) must equal the sum of the fluxes of the cations leading to oxide formation (the oxide formation flux) and those leading to dissolution (the dissolution flux).

Our MCB model considers that the full corrosion system consists of four elementary steps, electrochemical reaction (metal oxidation coupled with reduction of aqueous species), transport of charged species through the oxide layer, dissolution of metal cations, and oxide formation, as schematically shown in Fig. 2 in our paper (due to mass and charge conservation, only three flux equations needed to be formulated). Since these steps are not independent but coupled processes, it is not necessary to define a rate-determining step. The mass and charge balanced rate equations will automatically adjust the overall corrosion rate to the rate dictated by the rate determining step, and the rate step can change depending on the corrosion conditions. The physical parameters needed to calculate the kinetics of oxide growth are listed in Table 1 of our paper. They are fundamental parameters or independently measurable parameters, including:

- equilibrium potentials for redox reactions of metal/metal oxide that can occur on a given alloy,
- specific (*i.e.*, linear) potential drop across an oxide,
- first-order rate constants for oxide formation and dissolution, and
- activation energy for oxide growth.

The values of some of these parameters used for our simulation results are also listed in Table 2 of our paper.

Markus Tautschnig said: It is assumed in the presented model that the electric potential drop across the layer increases linearly with the thickness of the layer. What is the physical explanation and reasoning leading to this assumption?

Clara Wren answered: The oxide layer that is growing on a corroding surface is not likely a pure semiconducting layer. During corrosion there will be continuous injection of metal cations at the metal/oxide interface and oxygen anions at the oxide/water interface. Thus, our model assumes that the oxide layer is more likely a p–n junction in a solid-state diode device as shown in Fig. 5 of our paper. The potential drop across the oxide layer resembles a junction potential rather than the semi-conductor band-gap. The junction potential arises from the resistance to the diffusion of electrons and holes and hence increases with the diffusion length.

John Scully asked: Oxidation and insertion of metal cations at the metal oxide interface was modeled using a Butler–Volmer type expression originally aimed at charge transfer controlled oxidation. Why not consider using another expression, perhaps more suitable to the metal/oxide interface, such as those developed by Cabrera and Mott, Macdonald, Young or Sato?

Clara Wren responded: The Butler–Volmer equation is a more fundamental flux equation for interfacial charge transfer, but it requires knowledge of the potential difference between the metal and oxide phases at the metal/oxide interface. This potential difference is not defined as a function of more fundamental parameters in the other models, and hence, the expression for the overall interfacial charge transfer in other models includes the effects of the solution redox environment and the oxide potential barrier semi-empirically. In the MCB model, the potential drop across the oxide layer is defined as a function of the type and thickness of the oxide that is growing and the driving force for the interfacial transfer is defined as a function of equilibrium potential for the metal oxidation coupled with solution reduction (see Table 1 in our paper). Thus, the MCB model can calculate the potential difference at the metal/oxide interface, (this is referred to as the effective overpotential for metal oxidation in our paper). Consequently the MCB model does not need to use a semi-empirical formula and uses the more fundamental rate equation for the interfacial charge transfer.

Christopher Taylor opened a general discussion of the paper by Denis Kramer: The strains described in the paper were 2D and equally applied in those two dimensions. Have you investigated the role of uniaxial stresses on the adsorption energy and geometry of oxygen on copper? A relevant paper might be the work by Francis and Curtin, "Mechanical work makes important contributions to surface chemistry at steps".[1]

1 M. F. Francis and W. A. Curtin, *Nat. Commun.*, 2015, **6**, 6261.

Denis Kramer answered: We have not yet considered an anisotropic strain, but agree that this is a very interesting topic.

Christopher Taylor questioned: Can you please further elaborate upon what the two peaks C1 and C2 in the signals for the cyclic voltammetry correspond to when strain is applied? Why does strain introduce a second peak?

Denis Kramer replied: The two peaks are assigned to two different adsorption modes of an oxygen species, one showing higher sensitivity towards strain than the other. Our modelling results suggest that C2 might be attributable to the unreconstructive adsorption mode as we find higher sensitivity of unreconstructed adsorption of oxygen towards strain than for reconstructive adsorption.

David Shoesmith asked: Is it possible that the introduction of sufficient strain into the Cu surface could lead to its susceptibility to corrosion in anoxic water?

Denis Kramer answered: Straining Cu will add mechanical energy to the Gibbs free energy of the solid, in principle shifting the stability windows of the metal. We, however, do not expect this thermodynamic effect to be very pronounced and think that secondary effects need to be considered. This includes the influence of the strain state on the adsorption energies of intermediates and related kinetic barriers of the corrosion reaction. Unfortunately, our results presently do not provide the opportunity to speculate on kinetic effects due to the stress state of the surface.

Vincent Maurice commented: The discussion of the CVs (Fig. 5 in your paper) appears not relevant for a (100) surface. As described, the surface preparation does not include the final stage that allows recrystallising the cold work layer formed by mechanical polishing. As a result, the topmost surface will not have exposed (100) planes but instead a highly defective structure.

Denis Kramer answered: A commercially available polished Cu single crystal oriented along [100] was used for the study. We agree that further pretreatment would have necessitated a reassessment of the surface orientation. This, however, was not the case and the single crystal was used as received. The good agreement with our *ab initio* modelling provides further corroborating evidence. Hence, we belief the interrogated surface to be reasonably representative of Cu(100).

Vincent Maurice further commented: The DFT-derived surface Pourbaix diagram for the unstrained Cu(001) only partially reproduces the available experimental data obtained at pH 13.[1] In this work, adsorption-induced surface reconstruction was indeed observed some 700 mV before 3D bulk oxide growth. However, the observed superstructure was *c*(2x6) and not $(2\sqrt{2}\text{x}\sqrt{2})\text{R45}^\circ$ as modelled in the present paper for pH 13. Even if the atomic model proposed for the *c*(2x6) may not be fully correct, we note from Table 2 in your paper that its energy is below that of the unreconstructed adsorbed structure for OH adsorption that must be considered at alkaline pH.

1 J. Kunze, V. Maurice, L. H. Klein, H.-H. Strehblow and P. Marcus, *J. Electroanal. Chem.*, 2003, **554–555**, 113–125.

Denis Kramer replied: We agree that the (100) surface is likely to reconstruct in aqueous environments. Although we explicitly considered the reconstruction proposed by Kunze *et al.*,[1] we were unable to identify any OH super-structure using DFT that would be thermodynamically stable within reasonable bounds of pH and voltage. We do not exclude that an exhaustive search through all possible atomic arrangements within a *c*(2x6) supercell might be able to identify a thermodynamically stable OH-terminated configuration. Indeed, our results encourage the development of a refined model of the reconstructive OH adsorption mode as we predict reconstructive adsorption of O and OH to be energetically more favourable relative to their respective unreconstructed adsorption modes.

1 J. Kunze, V. Maurice, L. H. Klein, H.-H. Strehblow and P. Marcus, *J. Electroanal. Chem.*, 2003, **554–555**, 113–125.

Philippe Marcus asked: On Cu (111), combining *in situ* STM determination of the adsorbed overlayer structure, and electrochemical measurements of the charge passed during adsorption, it was shown that the adsorbed species (at pH 13) was OH, and not oxygen. Why would it be so different for Cu (100)?

Denis Kramer responded: Please see the answer to the previous question by Vincent Maurice. Further, our study focused on mildly acidic conditions (pH 5) where experimental evidence for adsorption of oxygen at Cu(100) within the missing row reconstruction was provided by Cruickshank *et al.* (*cf.* ref. 12 in our

paper). Cruickshank *et al.* also pointed out that this is markedly different from Cu(111). The prevalence of O as opposed to OH as the adsorbing species in acidic media is further supported by surface-enhanced Raman spectroscopy (SERS) data from Chan *et al.* (*cf.* ref. 27 in our paper).

Hendrik Bluhm remarked: How well is the surface structure, crystallographic orientation and cleanliness controlled in the experiment? In particular, what is the miscut of the (001) orientation and how does this influence the terrace size/step density?

Denis Kramer answered: Please refer to the answer to the previous question asked by Philippe Marcus.

Rob Lindsay said: I was wondering if you have any strong evidence that the surface terminations you theoretically predict are present in your experimental measurements, *i.e.* have you conducted any characterisation beyond cyclic voltammograms. If not, it would be very interesting to do so, perhaps using surface diffraction, as it is possible that the surface terminations are more complex than suggested.

Denis Kramer replied: We fully agree that further sophisticated studies of the precise atomic arrangement at the interface under various conditions would be highly beneficial and likely to bring new insights.

Simon Gibbon addressed Denis Kramer: In your experiment the strain is induced by a spherical ball being pressed into the copper sheet. I would expect this to induce a radial strain field in the copper surface and that the surface reorganisation of the copper atoms may be different from surface reorganisation caused by a strain in the *x*-direction followed by a subsequent (or even simultaneous strain) in the *y*-direction. In your modeling work, how has the strain been applied?

Denis Kramer answered: We did not consider the radial nature of the strain within our atomistic modelling due to the difference in length scales between the atomistic domain and the radius of the electrode. Isotropic strain was introduced in the modelling work by scaling the lattice constants appropriately.

Clara Wren remarked: In your DFT calculations, what was the functional used? How did you introduce the stress in the DFT calculations? How do you model the interface where the periodicity of wave function ends, and how do you model the effect of the stress on the functional?

Denis Kramer replied: We used the Generalised-Gradient-Approximation (GGA) to DFT in a parameterisation due to Perdew, Burke, and Ernzerhof (PBE). Stress was introduced by straining the lattice constants. The wave functions were expanded in a plain-wave basis making the consideration of basis set superposition errors (BSSE) irrelevant. Further, we only sampled a single *k*-point perpendicular to the surface to minimise spurious interactions between slab images. We have not considered any influence of the stress on the functional itself. Note that only the exchange–correlation term of the functional is not

precisely known and needs to be parameterised. While there are interesting approaches to improve the predictive power of PBE for adsorption phenomena (*e.g.*, the revised PBE out of the Norskov group), we are not aware of any work explicitly considering strain as part of the parameterisation of the exchange–correlation term.

Mira Todorova asked: There should be two in-equivalent adsorption geometries at 1/2 ML oxygen coverage on Cu when the system is under strain, due to the significant rumpling of the surface (*cf.* Fig. 2 of your paper). In one of them the coordination of O should be increased (structure shown in Fig. 2). Am I correct in assuming that this is the geometry which is affected when the structure is strained, while the energy of the other structure remains unchanged, regardless of the strain state?

Denis Kramer responded: The substantial rumbling was only seen for O adsorption at the top site. The rumbling is not a direct consequence of straining the surface. It is induced by the adsorption of oxygen. Straining the clean surface as well as a full ML of O did not lead to rumbling. We, therefore, report the adsorption energy of O at the recessed Cu atoms only.

Geoffrey Thornton commented: Scanning tunnelling microscopy does not have sufficient lateral resolution to detect tensile strain of a few percent on Cu(001). However, X-ray scattering does provide a potential route to measure the strain.

Julian Wharton replied to the comment: Yes we agree that the combination with more advanced refractive and/or scanning probe characterisation would be very beneficial to provide further experimental evidence.

Anton Kokalj communicated: The explanation that the $(2\sqrt{2}\times\sqrt{2})R45^\circ$ missing row (MR) reconstruction on Cu(100) is driven by compressive stress induced by chemisorbed oxygen is plausible, and calculations performed with imposing 2% tensile strain nicely confirm the argument. Nevertheless, I believe there is a deeper reason behind the MR reconstruction, which is actually confirmed and strengthened by the current stress argument. (We have investigated the MR reconstruction of O/Cu(100) and O/Ag(100) systems[1] and structurally related step-edge decoration of oxygen on Ag(410)[2] by DFT calculations; more details about the below given explanation for the stability of MR can be found in ref. 2.)

In the MR reconstruction oxygen atoms are fully decorating step-edges by forming the –O–Cu–O–Cu– chains. These oxygen atoms are sunk into the surface, *i.e.*, oxygen and Cu atoms are almost aligned, if looked at along the step-edge direction. Hence, they form the structure of stable electrostatic +−+−+−+− strings. Indeed, in this structure oxygen atoms are particularly stable. This reasoning is confirmed by calculation with 50% of O atoms removed, such that step-edge displays the –O–Cu–Cu–O–Cu–Cu– structure. The corresponding magnitude of adsorption energy is considerably reduced with respect to 100% decorated step-edge, because the above mentioned electrostatic stabilization is not operational in this case.

So what happens is this: in the parent structure, $c(2\times2)$–O/Cu(100), oxygen atoms would like to sink into the surface so that repulsive lateral interactions between negatively charged O adatoms would be screened. But they cannot do so, because they are too big (actually they are able to do it only slightly and this is the origin of the observed oxygen induced compressive stress). In contrast, in the MR structure, the O atoms have more space due to missing Cu atoms and they can sink into the surface to become electrostatically stabilized as explained above.

1 N. Bonini, A. Kokalj, A. Dal Corso, S. de Gironcoli, and S. Baroni, *Surf. Sci.*, 2006, **600**, 5074–5079.
2 N. Bonini, A. Kokalj, A. Dal Corso, S. de Gironcoli, and S. Baroni, *Phys. Rev. B: Condens. Matter Mater. Phys.*, 2004, **69**, 195401.

Denis Kramer communicated in reply: We agree that coulomb screening is a likely fundamental process influencing the observed phenomena, which is in full agreement with our findings and interpretation.

Mary Wood opened a general discussion of the paper by Vincent Maurice: Concerning the TOF-SIMS data presented in Figure 1 of your paper, how do you compensate for the different relative sensitivities of the different elements of interest to the technique? As far as I am aware, relative sensitivity factors (RSFs) have only been reported for trace elements within a matrix, such as silicon, making it difficult to apply to a system such as steel. However, these RSFs indicate that whilst nickel and iron show comparable sensitivity, chromium has a sensitivity that is generally around an order of magnitude higher, and oxygen has a sensitivity around three orders of magnitude lower. I was wondering how significant you expect these factors to be in this case?

Vincent Maurice replied: In Figure 1 of our paper, the relative intensities of the selected ions cannot be regarded as indicative of their concentration. O^- ions have a high ionisation yield when emitted from an oxide matrix. Here, the lower intensity $^{18}O^-$ isotope is reported since $^{16}O^-$ had an intensity close to saturation of the detector. The Fe^{2-}, Ni^{2-}, and Cr^{2-} negative ions have a relatively low intensity when emitted from a metallic matrix (positive ions have a higher ionisation yield for metallic ions but it is not possible to reverse the polarity during the depth profile). We have no calibration data of the RSFs for these ions in a metal matrix that would allow determining their relative concentrations. We emphasize that the quantification of the elemental concentration in the alloy was done using the XPS intensity data, not the ToF-SIMS data.

Rob Lindsay remarked: Your ToF-SIMS data suggest that O/OH species are present in the substrate. Could you comment on this result?

Vincent Maurice answered: We see this as a possible artefact effect of the surface analysis by the primary ion beam. Even though the extremely low primary ion dose used corresponds to static SIMS analytical conditions, the impinging ions create atomic plane mixing by pushing the target atoms below the topmost surface plane from which the secondary ions are mostly emitted. With continuous depth profiling, this effect continues even after entering the substrate region leading to the measurement of high intensity tails in the profiles.

Jonathan Morrison commented: In our own studies of the corrosion of 316L stainless steel under high temperature water conditions, we've seen that molybdenum has almost no effect on the oxide film, and is instead dissolved into solution. Have you performed a mass balance calculation to be certain that all of the molybdenum in your experiments has been retained in the oxide films, or to determine the total loss of molybdenum to the solution? How can you be certain that the molybdenum in your films represents the total amount present at the beginning of your test?

Vincent Maurice responded: The total amount of oxidized Mo present in our native oxide film is 2.1% of the total cation fraction in an oxide matrix 1.7 nm thick. After 2 h passivation, this amount increases to 3.6% of the total cation fraction in an oxide matrix 1.9 nm thick. This shows that not only the Mo initially present has been retained in the passive film but also that Mo enrichment took place, implying Mo consumption from the alloy substrate. Of course, one cannot exclude some Mo loss to the solution during passivation, implying an even higher consumption of Mo from the alloy. However, our data show no significant variation of the metallic Mo at the alloy surface.

Hiroki Habazaki questioned: Do you have some results on the potential dependent film composition and film structure? Mo(IV) is stable at low potentials close to the active dissolution region of stainless steel. So, the composition and film structure may change with potential.

Vincent Maurice answered: The potential dependence of the film composition and Mo(IV)/Mo(VI) balance has not been studied in the work reported here. From *in situ* STM data (to be published), the film nanostructure was found to be potentially dependent with the weaker sites continuously enlarged by dissolution for polarization in the pre-passive range before time-assisted curing promoted by the presence of Mo in the alloy.

Gerald Frankel asked: You have made several observations regarding the effect of Mo. Can you speculate as to which is the most important in conferring corrosion resistance?

Vincent Maurice replied: Two of the observed Mo effects, strong Mo(VI) enrichment after passivation and Mo-assisted curing of the weak sites, appear as linked. Mo(IV) present prior to passivation (2.5% of the cations in the inner layer 1 nm thick) is still present after passivation (3% of the cations in the outer layer 0.6 nm thick) and not enriched. In contrast, Mo(VI) gets markedly enriched (increasing from 1.0% initially to 7.9% after passivation). At the same time, Mo is observed to assist curing of the weak sites of the passive film revealed by transient dissolution and hence to likely concentrate as Mo(VI) in these weak sites. It does not exclude that Mo(VI) could also be present in the oxide matrix where no weak sites were revealed by transient dissolution but where a similar Mo(VI) enrichment/curing mechanism could operate but at a smaller scale, *e.g.* in the intergranular sites of the oxide matrix. Thus, this combined effect of Mo(VI) enrichment and curing of weak sites appears as most important for increasing the

corrosion resistance in the passive state and in the initiation of localized corrosion for which the presented data are relevant.

Clara Wren commented: The passivation potential that you used in your experiments was 0.5 V, a very oxidising potential. The corrosion potentials on Ni–Fe–Cr alloys even in the presence of O_2 and H_2O_2 are not likely to reach that high a potential. Could you comment on whether the oxide structure that you see at such a high polarization potential can be extrapolated to the oxide structure that can be formed on naturally corroding surfaces? What are the equilibrium potentials for Mo to Mo(IV) and Mo(IV) to Mo(VI) conversion? Do you expect to form Mo(VI) oxides/hydroxides at the high polarization potential? What are the solubilities of the Mo(IV) and Mo(VI) hydroxides? Do their solubilities support your proposed oxide structure?

Vincent Maurice responded: A revisited Pourbaix diagram of the Mo-H_2O system at 25 °C, including the many forms of molybdates, has recently been proposed.[1] It shows that, in our passivation conditions (0.5 V/SHE, pH 1.3, RT), the Mo(VI) oxide phase (MoO_3) is the most stable expected, the Mo(IV)–Mo(VI) transition being in the 0.25–0.33 potential range at pH 1.3. Our results that show passivation-induced enrichment in Mo(VI) only (see also answer to the previous question asked by Gerald Frankel) are thus consistent with this prediction. However, this diagram also shows that the solubility limit for the formation of polymolybdates ($H_2Mo_8O_{26}^{2-}$) is pH = 1.9 +0.5 log a. Thus at pH 1.3, one can expect the transpassive dissolution of polymolybdates (0.07 M) and speculate their redeposition on the surface. A Mo enrichment of the passive film dominated by the formation of Mo(IV) species at lower potential has not been studied in the present work. Still, the experimental conditions of our model study are relevant for pitting initiation in the middle of the passive range as expected for a Mo-bearing alloy in chloride-containing environments.

1 P. A. Nikolaychuk and A. G. Tyurin, *Butlerov Communications*, 2011, **24**, 101–105.

Frank Renner remarked: My research group has recently addressed the corrosion and dissolution behavior of a stainless-type amorphous steel ($Fe_{50}Cr_{15}Mo_{14}C_{15}B_6$) and its respective partially and fully nanocrystalline derivates.[1–3] For the amorphous alloy a very flat and homogeneous Cr-rich passive oxide forms due to the ideal homogeneous distribution of the elements in the amorphous structure and the flat starting surface. With an increasing degree of (partial) crystallization this initially amorphous alloy forms Cr-depleted Mo-rich nanoscale crystallites which dissolve preferentially creating a nanoscale roughness of the forming Cr-rich passive film. This roughness (see Fig. 1) translates directly to respectively higher steady state dissolution. As a direct conclusion of this work we therefore realized the importance of the nanoscale morphology of the passive films on the relative stability of the alloy.

Do you have more information or can you speculate on the elemental composition of the different (lower and higher) patches visible on your surfaces? Does the surface morphology of your passive oxide change with time and do you observe a similar influence of changing surface morphology on the passive current, *i.e.* the steady-state dissolution rate?

1 M. J. Duarte, J. Klemm, S. O. Klemm, S. Borodin, K. Mayrhofer, M. Stratmann, A. H. Romero, D. Crespo, J. Serrano, P. Choi, D. Raabe and F. U. Renner, *Science*, 2013, **341**, 372–376.
2 M. J. Duarte, A. Kostka, J. A. Jimenez, P. Choi, J. Klemm, D. Crespo, D. Raabe and F. U. Renner, *Acta Mater.*, 2014, **71**, 20–30.
3 J. Klemm, M. J. Duarte, S. O. Klemm, P. Choi, K. J. J. Mayrhofer and F. U. Renner, *Corros. Sci.*, 2014, **89**, 59–68.

Vincent Maurice responded: It remains unknown from our present data for this system if the nanogranular morphology of the matrix of the oxide film revealed by STM presents variation of composition between grains or even in-between them (at the interface between grains). A recent conductive AFM study performed in our group on thicker passive films with larger grains formed on 316L stainless steel in simulated PWR water at 325 °C led to the conclusion that, indeed, there are variations of the oxide composition on different grains and in-between them.[1] As discussed previously (answer to the question asked by Gerald Frankel), one could speculate that Mo(VI) enrichment could also take place in the weaker (*i.e.* intergranular) sites of the observed matrix by a local dissolution-induced mechanism similar to that revealed at larger scale in the present study. Certainly, *in situ* monitoring of the time evolution of the granular morphology of the oxide matrix and its relation with the passive current appears relevant for future work in that prospect.

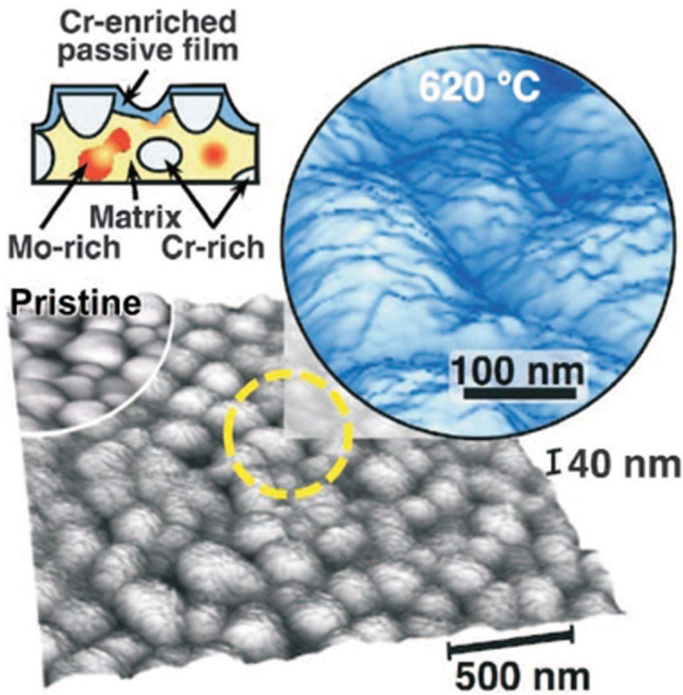

Fig. 1 AFM image of a partially nanocrystalline derivate of a stainless-type amorphous steel ($Fe_{50}Cr_{15}Mo_{14}C_{15}B_6$) after polarization in the Cr-dominated passive regime in 0.1 M H_2SO_4. Nanoscale roughness develops by selective dissolution of Cr-depleted Mo-enriched phases and results in a higher passive current. Adapted from ref. 1.

1 T. Massoud, V. Maurice, F. Wiame, L. H. Klein, A. Seyeux and P. Marcus, *Corros. Sci.*, 2014, **84**, 198–203.

Alison Davenport enquired: How do you think that Mo prevents localised corrosion of stainless steel? There is well-established evidence that it decreases the rate of propagation of pits by decreasing the rate of active dissolution (*e.g.* ref. 1). How might the effect of Mo on the passive film affect localised corrosion susceptibility?

1 R. C. Newman, *Corros. Sci.*, 1985, **25**, 331.

Vincent Maurice answered: It is clear from the presented data that Mo plays a role in the initiation stage of localized corrosion by pitting. Not only Mo is found strongly enriched (as Mo(VI)) in the passive film but it is found to act locally in the weak sites of the passive film where dissolution is preferential. It can be speculated that this beneficial effect will operate in the metastable pitting stage retarding pit initiation (see also my answer to the question previously asked by Gerald Frankel). This does not exclude that a Mo effect also operates in the pit propagation stage, by decreasing active dissolution.

Rob Lindsay remarked: Regarding the chemical nature of the Mo species incorporated into the outer part of the passive film, you suggest that it may be molybdate on the basis of its oxidation state (Mo(VI)). Under the acidic conditions of your experiments, would you expect polymolybdates to be present?

Vincent Maurice replied: The formation of polymolybdates by transpassive dissolution of Mo(VI) can be expected in our acidic solution as shown by a revised Pourbaix diagram for molybdenum (see answer to the previous question by Clara Wren). This implies a dissolution/redeposition rather than a solid state mechanism of formation, in which case the formation of polymolybdates bonded to Fe cations appears as a sound possibility since Mo(VI) is found in the Fe-rich outer part of the passive film.

David Shoesmith addressed Vincent Maurice and Philippe Marcus:Your results appear to confirm that Mo has no observable role on the properties of the passive film and that its primary function is to repassivate a very large number of metastable pitting events. This is consistent with our observations on Ni–Cr–Mo alloys (which contain considerably more Mo than the steel used in your experiments). Is the evidence you generate enough to confirm that the primary function of Mo is to form oxidized (Mo(VI) states that reseal the passive film? If so, do your results rule out the claim that the primary function of Mo is to suppress the anodic oxidation of the alloy?

Vincent Maurice and **Philippe Marcus** jointly responded: Our data indeed support the view that a primary role of Mo (present in our model alloy at similar concentration as in 316L stainless steel) is to promote a reseal of the passive film by Mo(VI) enrichment (see also Vincent Maurice's answer to the previous question by Gerald Frankel). However, we do not exclude that Mo also decreases anodic

dissolution (see also Vincent Maurice's answer to the question previously asked by Alison Davenport).

Angus Cook asked: In Fig. 2 of your paper the ToF-SIMS data show that both the air passivated sample and the sample passivated potentiostatically for 20 h have similar intensity counts for the four secondary ion species surveyed when sputtering has reached the metal substrate (~400–500 s). The sample passivated potentiostatically for 2 h, however, shows a higher intensity reading at these sputtering times for all four secondary ions. Can you suggest a reason for this difference?

Vincent Maurice replied: This difference is also observed in Fig. 1 of our paper for all ions in the substrate region. A possible cause is that the low current (set to 1.3 pA) of the primary Bi^+ ions used for analysis may have varied in the different experiments. We emphasize that the quantification of the cation concentration was done using the XPS intensity data, not the ToF-SIMS data.

Rob Lindsay opened a general discussion of the paper by David Williams: Having begun some work in the area of CO_2 (sweet) oilfield corrosion, I have the impression that the literature is rather inconsistent, with many apparently simple questions outstanding. Do you agree with this opinion, and if so do you have any idea as to why this is so, beyond simply the complexity of the topic?

David Williams replied: I do agree with your opinion. As Professor Taylor's paper later in this Discussion will surely emphasise, corrosion is generally a complex, multi-faceted phenomenon, and it can be difficult to cut through to the basic processes that underly the behaviour. Often, to find these underlying processes needs new experimental techniques and we have been fortunate in that we have been able to deploy one such that turned out to be very appropriate for this study. We were also fortunate that in the course of developing this study we discovered the potentiostatic current transients that were correlated with the appearance of crystalline siderite. This was a complete surprise. We were then able to unravel a number of interacting effects.

John Scully asked: The notion of looking at the metal/solution interface and at the colloidal aspects of the solution at the same time *in situ* was particularly novel. What do you think was the effect of Cr on the crystallization and formation of Siderite?

I assume that the Cr that affected the process was in solution and came from the alloy. If this is the case, does that mean that the scaling processing depends critically on the Cr alloying content and the details of Cr release? This implies that every oil field alloy used pertinent applications will have subtle differences in behavior. Comments?

David Williams replied: I can only speculate as to the detailed mechanism of the Cr effect, which seems (on the limited evidence available) to be a general effect of highly-charged metal ions, which also includes Ca^{2+} and Mg^{2+} (references in our paper). The effects are on both the nucleation and growth of the amorphous colloid precursor and on its transformation to crystalline siderite. It might be that

these ions adsorb at the boundary of pre-nucleation clusters (ref. 50 and 51 of our paper). I agree that the observations could imply that the scaling might depend critically on the alloy composition and how the species such as Cr are released. The GI-SAXS/WAXS experiment is an extremely powerful method for revealing details of the initial stages of surface scale formation and as such would be very appropriate for exploration of the effects of alloy composition. One aspect of our experiment that was not under good control was the transport of species to and from the surface. An important extension of the experiment would be to redesign the cell so that the effect of flow in the solution could be studied in detail, which I think would then allow your question to be better addressed.

Christopher Taylor said: Can you speculate upon the mechanism by which Cr(III) influences the formation of these amorphous phases? Do you think it may be acting as a catalytic agent in the nucleation of the siderite? Can you also briefly describe Ostwald's rule of stages and how it applies here?

David Williams answered: Ostwald's rule of stages states: "As a stepwise reaction proceeds, it is not the state with lowest Gibbs energy that is initially obtained, but the least stable one, lying nearest to the original state in Gibbs energy".[1] As applied to crystallisation, this rule has been used to underpin a mechanism that postulates a succession of steps, from pre-nucleation clusters, through amorphous states to the crystalline state, rather than a classical nucleation mechanism which postulates a critical nucleus size determined by the balance of interfacial and bulk (volume) Gibbs energy. In the case of calcium carbonate nucleation, highly dynamic, liquid and chain-like polymers of calcium carbonate ion pairs have been proposed.[2] I note that there may be an analogy to the effect of silica on the formation of prenucleation clusters of $CaCO_3$, where adsorption of colloidal silica on the periphery of the clusters is proposed as a mechanism both for stabilising the clusters and promoting their cross-linking into aggregates.[3] In the present case, Cr^{3+} or colloidal chromium oxyhydroxide-carbonate may play a similar role.

1 R. A. van Santen, *J. Phys. Chem.*, 1984, **88**, 5768–5769.
2 R. Demichelis, P. Raiteri, J. D. Gale, D. Quigley and D. Gebauer, *Nat. Commun.*, 2011, **2**, 590.
3 M. Kellermeier, D. Gebauer, E. Melero-García, M. Drechsler, Y. Talmon, L. Kienle, H. Cölfen, J. M. García-Ruiz and W. Kunz, *Adv. Funct. Mater.*, 2012, **22**, 4301–4311.

Gerald Frankel questioned: Do you have any evidence that the mechanism for the effect of Cr on siderite formation is the same for Cr as an alloying element as for Cr^{3+} in solution?

David Williams responded: We recently presented in detail a study of the effect of Cr additions to the steel and in solution.[1] Fig. 2 compares the evolution of current density and diffraction peak intensity for two steels of the same quenched and tempered microstructure where one steel contains 1 wt% Cr and the other does not. Cr^{3+} is added to the solution at concentrations from 0 to 100 μM in the case of the steel that does not contain Cr. Addition of Cr^{3+} to the solution in this case shortens the induction time for scale nucleation, as shown by the occurrence of the peak in the current density and the appearance of the diffraction peaks for siderite and chukanovite. In the case of the Cr-containing steel, the nucleation of

a surface scale occurs almost instantaneously after initiation of the anodic reaction. The scale formed was very thin and adherent and there was some evidence for intergranular corrosion initiating.[1] Thus, there is a strong effect of Cr in the steel upon the nucleation and growth of the scale. It is an assumption that the mechanisms acting in the case of Cr in the steel and Cr in solution are similar. It is debatable whether Cr from the steel will be released into the solution or whether it forms a colloidal oxy-hydroxide immediately adjacent to the surface with this acting as seed for nucleation of the corrosion scale.

1 M. Ko, B. Ingham, N. Laycock and D. E. Williams, *Corros. Sci.*, 2014, **80**, 237–246.

David Shoesmith enquired: You observe the formation of chukanovite as well as siderite. Is this expected during pipeline corrosion? In groundwater systems whether siderite or chukanovite form tends to be determined by the relative concentrations of hydroxide and carbonate. Given that you see pH changes during film formation could this lead to chukanovite formation? Is it also possible that local changes in chemistry are a requirement for the Cr(111) effect. The high sensitivity to Cr(111) suggests this could be the case.

David Williams replied: I do not know whether chukanovite forms during pipeline corrosion. I suspect that, if it did, the scale morphology would be significantly affected and that the resultant scale would not be nearly as protective as siderite: that, however, is a guess. The formation of chukanovite in our

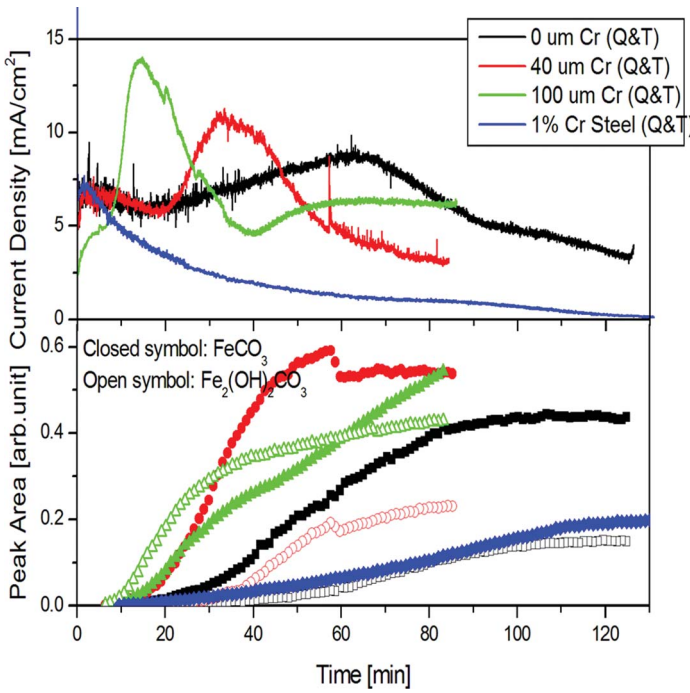

Fig. 2 Evolution of current density and diffraction peak intensity for two steels of the same quenched and tempered microstructure where one steel contains 1wt% Cr and the other does not.

experiments may indeed be a consequence of the pH changes that we deduce accompany siderite crystallisation, because usually the formation of chukanovite follows that of siderite and seems to be more pronounced the more rapidly siderite is formed. We also hypothesise in the paper that the transport of Fe^{2+} through the amorphous surface 'gel' could form an iron-rich gel that could be considered as an amorphous chukanovite. We hypothesise that the effect of Cr^{3+} is representative of a general effect of high-valent metal ions, based on our own observations of the effect of La^{3+} on the crystallisation rate[1] and on literature suggestions cited in our paper that the crystallisation of amorphous ferrous carbonate is sensitive to the presence of traces of Fe^{3+}.

1 M. Ko, B. Ingham, N. Laycock and D. E. Williams, *Corros. Sci.*, 2014, **80**, 237–246.

Gaurav Joshi commented: Having performed 6-day immersion corrosion experiments on polished pure Fe (macroelectrode (0.8 cm^2)), which was allowed to remain at OCP in $CO_{2\text{-sat}}$ water (across a range of [NaCl] @ 80 °C, pH 6.8 (comparable to the experimental conditions in your paper)), I present some data which might support the conclusions of your paper (amorphous siderite), in particular, to lines 40–41 on page 15, "presence of a discontinuous layer comprising 'blobs' of amorphous $FeCO_3$". Between regions of discrete crystalline siderite crystals, where the surface appears only to have suffered uniform corrosion, high resolution imaging in secondary electron and back-scatter electron mode in SEM indicate only a roughened surface. However, as the working distance and accelerating voltage are lowered, and the detector changed to one located within the electron beam column (annular), some darker string-like features are clearly elucidated. These have a lower electronic work function than the conducting Fe substrate and are suspected to be nanocrystalline strings/blobs of iron carbonate. *Ex situ* micro-Raman spectroscopy from such regions reproducibly provides a broad peak in the range 400–700 cm^{-1}, centered at 620 cm^{-1} and shoulders at 520 cm^{-1} and 690 cm^{-1}. These shoulders are interpreted to separate into contributions from Fe–O stretches from siderite (520 cm^{-1}) and magnetite/maghemite (690 cm^{-1}), but the central peak (620 cm^{-1}) has to remain unassigned at this point. Carbonate stretches may not have been detected due to the nano-crystalline structure (molecular vibration constraints, perhaps?) or high fluorescence of the substrate. Complementary work with FT-IR and higher resolution techniques (*e.g.* AFM-IR) might assist in resolving/revealing their nature. Please refer to ref. 1. In ref. 1, the idea of colloidal solution forming close to steel substrate has been made (in passing) on page 5.

1 A. Dugstad, *Mechanism of protective film formation during CO_2 corrosion of carbon steel*, NACE International, Corrosion 98, paper no 31, 1998.

Tom Majchrowski asked: In your paper you suggest formation of corrosion protective siderite scales that nucleate within a surface gel of amorphous carbonate. You also mentioned a positive effect of chromium ions on the film growth. Would you be able to elaborate in more detail on the nature of the bonding within the surface film? Is it covalent or ionic? Does the intermolecular interaction play an important role in maintaining the film's structure?

David Williams responded: I assume that the amorphous iron carbonate has similar bonding to amorphous calcium carbonate, and is a random hydrated ionic network. There is an extensive literature on amorphous calcium carbonate (references in our paper). Studying the bonding in these systems (*e.g.* by EXAFS) is difficult, because they are formed as a dilute colloid that is unstable to crystallisation.

Matthew Acres questioned: What chemical characterisation techniques, if any, were performed to distinguish the amorphous iron carbonate gel from a layer of atmospheric contamination?

David Williams answered: Chemical characterisation is extremely difficult for these thin surface layers that are also likely to transform if removed from the environment in which they are formed, and so we have not been able to do that. We can definitively state, however, that the species we detect form as a consequence of the anodic electrochemical reaction in the cell, because their appearance correlates with the current flowing.

Christopher Taylor queried: Can you determine if the nucleation of the siderite precipitate is heterogeneous (catalyzed by defects or otherwise on the surface of the material) or homogeneous (occurs in the aqueous phase, or in the near-surface aqueous phase)? How adherent are these films? If they are homogeneously nucleated, I would expect them to be less adherent since a direct bond between the surface and the film would not be anticipated.

David Williams responded: We have not detected the formation of crystalline siderite from the colloidal precursor in the solution or in the material deposited on the Kapton windows of the cell: Fig. 6 in our paper demonstrates that colloidal material was deposited or formed on and adhered to the cell windows, but there was no detectable WAXS signal from this material. Our GI-SAXS results imply, as we discussed, that crystalline siderite forms within an amorphous gel layer on the electrode surface, and we speculated on the possible importance of the gradient of Fe^{2+} concentration through the gel layer. This idea has elements of both homogeneous and heterogeneous nucleation. In some experiments, we replaced the Kapton window of the cell with a thin (1 μm thick) Fe foil in an attempt to see whether deposition of colloidal material from solution onto an iron surface was more efficient that on Kapton and whether it led to formation of crystalline siderite, but did not observe any crystalline material.

Rob Lindsay remarked: From reading your paper, I believe you have anodically polarised your sample to encourage scale growth on a shorter timescale. Have you attempted to undertake similar measurements at OCP? If so, what is the impact on scale formation, *e.g.* do you still see evidence for amorphous gel formation?

David Williams replied: We made one attempt to observe the surface film formation at the open circuit potential, by a transmission SAXS/WAXS experiment through a thin iron foil. Unfortunately, we did not vary the beam position during the 3 h run, so the X-ray beam carbonised the Kapton film that was backing the

iron foil and the Kapton film that formed the opposing side of the cell. There was no detectable WAXS signal from the crystalline material. We could not distinguish any SAXS signal that might have been due to a surface layer from a signal due to the amorphous carbon and we did not scan the beam over other parts of the Fe foil after the exposure. We had not at that stage suspected or detected the surface amorphous film, which we only found after we analysed our data in detail as described in the paper. This sort of blurred decision making often accompanies long sleepless stretches of synchrotron time. We will have to make a new beamtime proposal.

Rob Lindsay opened a general discussion of the paper by Frank Renner: According to your paper, the Cu_3Au (111) sample is prepared in UHV and then exposed to the ambient laboratory atmosphere before being patterned. Could you comment on the surface composition/structure following this exposure, *i.e.* how is the surface modified relative to that formed in UHV?

Frank Renner replied: The UHV prepared Cu_3Au (111) is found to be quite stable in ambient air. The sputter-annealing cycles in UHV produce a flat surface which is ordered according to earlier X-ray crystal-truncation-rod measurements up to the topmost atomic layer.[1] After a (short) exposure to air, some preferential oxidation of the topmost Cu occurs, which leads to an initial partial Cu dissolution on a thiol-free alloy surface even below the Cu equilibrium potential with immersion into the electrolyte. Yet, this procedure only showed the formation of a partial, not a full monolayer of Au, and *ex situ* AFM images of the alloy surfaces in ambient air show well-ordered atomic terraces. The adsorption of thiols then leads to Au segregation to the surface. There are no pronounced differences found in the surface morphology, even the surface exposed to ambient air for longer time before the fabrication of patterned structures. As a further comment important for the frequently necessary re-polishing step, we subjected the surfaces in-between the UHV treatment after fresh polishing to a gentle electrochemical etching step below the critical potential which lead to much smoother surfaces.[2]

1 A. Stierle, A. Steinhäuser, A. Rühm, F. U. Renner, R. Weigel, N. Kasper and H. Dosch, *Rev. Sci. Instrum.*, 2004, **75**, 5302.
2 (G. N. Ankah, A. Pareek, S. Cherevko, A. A. Topalov, M. Rohwerder and F. U. Renner, *Electrochim. Acta*, 2012, **85**, 384).

Rob Lindsay further asked: Regarding substrate templating, you indicate that you have sometimes pressed the stamp slightly harder onto the surface. Could you clarify what is the result of this harder pressing (*e.g.* are you simply enlarging the surface area contacted by the liquid)?

Frank Renner responded: Indeed, by hard-pressing we enlarge the contact area. But we need to consider that the amount of solution or of dissolved thiol molecules at the side walls is apparently lower than at the direct contact area. At least the density of thiol molecules is lower within the additional area. Here, a lying-down thiol phase is observed.

Hendrik Bluhm requested: What can we potentially learn from other modes of scanning probe microscopy, such as friction force microscopy, on the early stages of corrosion, before the onset of detectable morphological changes?

Frank Renner answered: As a very short answer: we did not yet perform other modes of AFM such as friction force microscopy. But we do agree that the lateral surface friction behavior should reveal interesting insights on the stability of the different adsorbed thiol phases. In a currently started project, my research group will indeed follow such approaches and further include also force–distance curves.

Trevor Rayment asked: Have you given consideration to the electrochemical activity of the thiol layer, since in your experiment you need to start the experiments at low potentials where the alloy is stable but at low potentials the thiol monolayer will be reduced or made more mobile? There is a substantial literature on the electrochemical properties of thiols. Indeed there are studies of the UPD of Cu SAMs on gold which might be regarded as being in some ways the reverse of the dealloying that you are studying.

Frank Renner replied: The thiol layer is stable in the potential regime we applied here. Our initial potential is above the one required for a cathodic desorption of the thiol layer and the critical potential, which is roughly our anodic limit, is below the anodic oxidation of the adsorbed molecules. In fact we have studied the effect of a higher anodic pulse applied to a similar ethanethiol SAM-covered Cu_3Au surface[1] and did observe the full or partial removal of the thiol film which in consequence directly led to large changes in the observed nanoporous surface morphology. We did not address the influence of the UPD of Cu on the SAM in the process as we started in an initially Cu-free electrolyte and always increased the potential during the experiments.

1 G. N. Ankah, A. Pareek, S. Cherevko, J. Zegenhagen and F. U. Renner, *Electrochim. Acta*, 2014, **140**, 352.

David Williams addressed Frank Renner: I'm assuming that the thiol adsorbs on gold, and also, that the final nanostructure developed is sensitive to surface diffusion.[1] However, how does that translate into adsorption on the intermetallic compound Cu_3Au? Also, since thiol adsorbs on gold, as the dealloying proceeds, would there be some surface diffusion or desorption and readsorption of the thiol onto the developing gold nanostructure that would consequently impact the nanostructure development? Or does the thiol alter surface diffusion of gold and hence the coarsening of the nanostructure?

1 J. Erlebacher, M. J. Aziz, A. Karma, N. Dimitrov and K. Sieradzki, *Nature*, 2001, **410**, 450.

Frank Renner answered: In regard to the influence on the surface diffusion we do clearly see that while the dealloying or formation and coarsening of nanoporosity starts at nearly thiol-free parts of the surface, the thiol-covered parts show no sign of coarsening or nanoporosity. The thiols do thus indeed considerably alter the surface diffusion. On the other hand we have no sign of thiols diffusing into the forming pores which are producing fresh thiol-free surfaces

below the initial surfaces. A change in the surface diffusion of thiol-covered Cu-Au surfaces was much earlier proposed by Moffat and Bard[1] and becomes in our experiments nicely visible. In regard of the initial state after adsorption the surfaces show a segregation of about 2–3 monolayers of Au, *i.e.* the thiols do indeed preferentially adsorb to Au. This effect can be clearly observed by *in situ* X-ray diffraction because already a single monolayer of Au on Cu_3Au (111) has a different in-plane lattice parameter compared to the substrate, and the ultrathin Au film approaches the expected Au lattice for slightly thicker films as we have shown in earlier work.[2–3] The adsorption of thiol molecules results in the formation of vacancy islands or ad-islands. These two features depend significantly on the various factors, *e.g.* stress on the Au surface due to thiolate molecules, molecular structures with or without a flexible alkyl spacer between the docking group and the aromatic backbone. The molecules used in this study are less flexible and introduce more stress on the substrate, which eventually leads to the formation of gold ad-islands. For the case of a less flexible system, these gold ad-islands are known to be quite mobile.[4]

1 T. P. Moffat, F. R. F. Fan and A. J. Bard, *J. Electrochem. Soc.*, 1991, **138**, 3224.
2 A. Pareek, G. N. Ankah, S. Cherevko, P. Ebbinghaus, K. J. J. Mayrhofer, A. Erbe and F. U. Renner, *RSC Adv.*, 2013, **3**, 6586.
3 A. Pareek, S. Borodin, A. Bashir, G. N. Ankah, G. A. Eckstein, M. Rohwerder, M. Stratmann, Y. Gründer and F. U. Renner, *J. Am. Chem. Soc.*, 2011, **133**, 18264.
4 W. Azzam, A. Bashir, P. U. Biedermann and M. Rohwerder, *Langmuir*, 2012, **28**, 10192.

Janine Mauzeroll asked two questions: 1. Did you consider using surface analytical IR methods to validate the thiol orientation giving the potential of non-negligeable interaction of the AFM tip in some of your results? 2. What is the achievable penetration depth with this dealloying method?

Frank Renner responded: We have so far indeed not used further techniques to address the different thiol structures. It is difficult to carry out the IR measurement on a patterned surface since the surface is not homogeneously covered with the target molecules. Also we see, as discussed in our paper, potential-dependent movements and formation of new standing-up thiol islands. However, we believe that in the patterned areas SAM molecules are densely packed and have no significant interaction with the AFM tip. We can further support the assumption of only weak interactions of the AFM tip with the thiol islands by SEM images of the same substrate or similarly treated surfaces which show no differences in the morphology between areas imaged by AFM and surrounding surfaces. The depth of homogeneous dealloying depends on the allied time and can reach from monolayers to complete bulk samples.

Rob Lindsay remarked: In Fig. 9 of your paper you demonstrate that adsorbed species can relatively easily interchange with those in solution. This result suggests that the adsorbed overlayers are rather dynamic in solution, *i.e.* adsorption/desorption events would be ongoing. On this basis, I am quite surprised that the templated substrates remain intact in solution. I would expect that the templating would become weaker as a function time through molecule desorption and adsorption at other locations. What is your expectation?

Frank Renner answered: We do see a slight out-diffusion of thiol molecules as we describe in our manuscript. Yet the effect is indeed not very strong which indicates in our view that the thiols are not frequently desorbed and re-adsorbed. The exchange mechanism then rather requires the displacement of one molecule by a molecule offering a more stable bond. Subsequently the same site triggers a growth of the more stable exchanged phase which may be called an intercalation process. It may here be illuminating to perform an exchange experiment on a patterned surface but we did so far only perform the patterning and the exchange in independent experiments as discussed in our present manuscript. The molecules in the early stage of adsorption or in the vicinity of the imprint are flat lying, poorly or less ordered and therefore may be more easily exchangeable.

Anton Kokalj communicated: How do the thiophenol and benzenoselenol molecules interact with the alloy surface, *i.e.*, only *via* the S and Se atoms or also with the benzene ring?

Frank Renner communicated in reply: Thiol and selenol moieties have a strong affinity to make a covalent bond to a gold surface and the benzene ring is then pointing upward also due to a low flexibility of the molecule (compare *e.g.* ref. 1).

1 M. Kind and C. Wöll, *Prog. Surf. Sci.*, 2009, **84**, 230.

